

ELECTROMAGNETIC MODELING OF SHIPS IN MARITIME SCENARIOS: GEOMETRICAL OPTICS APPROXIMATION

W. Fuscaldo^{1,2}, A. Di Simone^{2,3}, L. M. Millefiori², D. Riccio³, G. Ruello³, P. Braca², and P. Willett⁴

¹ Department of Information Engineering, Electronics and Telecommunications,
Sapienza University of Rome, 00184 Rome, Italy.

² NATO-STO Centre for Maritime Research and Experimentation, 19126 La Spezia, Italy.

³ Department of Information Technology and Electrical Engineering,
University of Naples “Federico II”, 80125 Naples, Italy.

⁴ Department of Electrical and Computer Engineering,
University of Connecticut, Storrs, CT 06269 USA.

ABSTRACT

Global Navigation Satellite System-Reflectometry (GNSS-R), is successfully employed for ocean altimetric and scatterometric applications. Recently, it has been suggested that GNSS-R can also be used for ship detection applications. To this purpose, an accurate electromagnetic modeling of the bistatic radar cross section of a ship lying over the sea surface would be very helpful. However, existing models are typically limited to monostatic configurations, thus restricting their applicability in multistatic scenarios, such as GNSS-R systems. In this work, we show a procedure to determine the bistatic radar cross section of a ship target, under the geometrical optics approximation. Numerical results show the impact of the geometry of acquisition and polarization on the bistatic radar cross section.

Index Terms— Electromagnetic scattering, geometrical optics, radar cross section, ship detection.

1. INTRODUCTION

Wide spatial coverage, accurate geo-localization, and ability to operate in all weather and day conditions are some of the main challenges of ship detection in the context of maritime surveillance [1]. Spaceborne systems for remote sensing, such as synthetic aperture radars (SAR) sensors and optical satellites are recently gaining much attention in this field [1, 2, 3].

Multistatic spaceborne systems, such as the Global Navigation Satellite System (GNSS), can profitably be used for ship detection [4, 5]. In fact, even if GNSS-Reflectometry (GNSS-R) is commonly used for ocean altimetric and scatterometric applications [6], it has recently been suggested that ship detection might be feasible under certain conditions [4]. While [4]

focuses on enhancing the signatures of ship targets in GNSS-R data, we discuss here the derivation of an accurate electromagnetic (EM) model of a ship in a maritime environment suitable for multistatic configurations.

Taking cues from [1, 7], where a rigorous theoretical framework has been developed for modeling the backscattering radar cross section (RCS) of ships in maritime environments [1], and buildings in urban scenarios [7], respectively, we extend the previous results to the most generic bistatic configuration. Specifically, a ship in open sea is here represented as a smooth dielectric parallelepiped lying over a rough surface [1] [see Fig. 1(a)-(b)]. Operating frequencies typically employed in such remote sensing systems allow for modeling the scattered fields under the Kirchhoff Approximation (KA), with a consequent great simplification of the scattering problem.

In this work, we evaluate by analytical and numerical means the bistatic RCS of a ship in a maritime scenario, under the geometrical optics (GO) approximation. This further approximation allows for clearly distinguishing the different contributions arising from multiple bounces between the sea surface and the ship hull. In particular, we focus on the double-bounce contributions [e.g., sea-to-hull, and hull-to-sea, see green dashed and solid lines of Fig. 1(b), respectively] since they turn out to be the most relevant ones [7]. Furthermore, the material composition and typical size of the ship, as well as the geometry of acquisition (namely, transmitter, scatterer, and receiver relative positions, and ship orientation), sea state, salinity and temperature, polarization of the incident wave and sensor resolution are accounted for.

2. THEORETICAL FRAMEWORK

From the definition of radar cross section (RCS)

$$\text{RCS} = \lim_{r \rightarrow \infty} 4\pi r^2 |\underline{E}_s|^2 / |\underline{E}_i|^2, \quad (1)$$

This research has been funded by the Office of Naval Research under contract N00014-16-13157, and this support is acknowledged with thanks to John Tague and Michael Vaccaro. There is parallel support to ONR-Global.

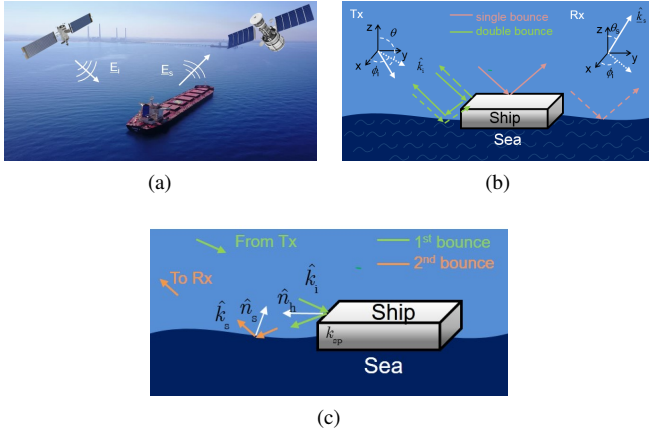


Fig. 1: (a) Representation of the scattering phenomenon under investigation: radar signals are scattered from a ship in open sea. (b) EM modeling of the scene represented in (a): the ship is represented as a parallelepiped, whereas EM waves propagate as rays according to the GO approximation. Green lines represent the double-bounce contributions: solid lines for hull-to-sea and dashed lines for sea-to-hull. Pink solid lines represent the single-bounce contributions: solid lines for ship returns and dashed lines for sea returns. In (c) the double-bounce contribution is modeled according to KA-GO.

it is manifest that the scattered electric field \underline{E}_s is required for the evaluation of the RCS. Here we assume that the incident field \underline{E}_i is a plane wave (due to the far-field distance between the scatterer and the satellites) with amplitude E_0 , polarization \hat{e}_i , and propagation direction \hat{k}_i [the hat ($\hat{\cdot}$) identifies unit vectors]:

$$\underline{E}_i = E_0 \hat{e}_i \exp(jk \hat{k}_i \cdot \underline{r}), \quad (2)$$

where k is the free-space wavenumber and \underline{r} the observation point. The field \underline{E}_s scattered by a possibly rough surface at the interface between two different homogeneous media is given, under KA-GO by [7]:

$$\underline{E}_s(\underline{r}) = \frac{jk e^{jk r}}{4\pi r} E_0 (\underline{I} - \hat{k}_s \hat{k}_s) \underline{F}(\hat{k}_i, \hat{e}_i, \hat{n}_s) \iint_S e^{j\eta \cdot \underline{r}'} d\underline{r}', \quad (3)$$

where $r = |\underline{r}' - \underline{r}|$ is the Euclidian distance between the surface \underline{r}' and the observation \underline{r} points, respectively; $\eta = \underline{k}_i - \underline{k}_s$, \underline{k}_i and \underline{k}_s are the incident and the scattered wavevectors, respectively, whereas \hat{n}_s is the surface normal unit vector that must obey the condition of specular reflection dictated by the stationary phase points (see Eq. (3.16) in [7]). The vector function \underline{F} depends on the surface slopes and dielectric properties; its expression is provided in [7] and is not reported here for the sake of brevity.

In order to have a more compact expression, it is convenient to express Eq. (3) in matrix form, e.g., by projecting \underline{E}_s onto the horizontal and vertical polarization states of the

scattered fields, so that Eq. (3) can be written as

$$\begin{bmatrix} E_{Sh} \\ E_{Sv} \end{bmatrix} = \frac{jk e^{jk r}}{4\pi r} \underline{S} \begin{bmatrix} E_{0h} \\ E_{0v} \end{bmatrix} \iint_S e^{j(\underline{k}_i - \underline{k}_s) \cdot \underline{r}'} d\underline{r}', \quad (4)$$

where the generic element S_{pq} of the scattering matrix \underline{S} is

$$S_{pq} = \left[(\underline{I} - \hat{k}_s \hat{k}_s) \underline{F}(\hat{k}_i, \hat{e}_{ip}, \hat{n}_s) \right] \cdot \hat{e}_{sq}, \quad (5)$$

with \hat{e}_{ip} and \hat{e}_{sq} for $p, q \in \{h, v\}$ being the incident and scattered polarization unit vectors, respectively:

$$\hat{e}_{ih} = \frac{\hat{k}_i \times \hat{z}}{|\hat{k}_i \times \hat{z}|}, \quad \hat{e}_{iv} = \hat{e}_{ih} \times \hat{k}_i, \quad (6a)$$

$$\hat{e}_{sh} = \frac{\hat{k}_s \times \hat{z}}{|\hat{k}_s \times \hat{z}|}, \quad \hat{e}_{sv} = \hat{e}_{sh} \times \hat{k}_s. \quad (6b)$$

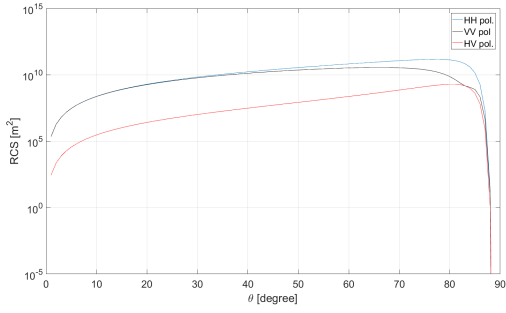
From the definitions above, it is clear that the bistatic RCS of a target under KA-GO is uniquely determined once the geometry of acquisition (affecting the calculation of both \underline{S} and the surface integral through \hat{k}_i , \hat{k}_s , and \hat{n}_s), as well as the material composition (affecting the calculation of \underline{S} through \underline{F}) and the size (affecting the calculation of the surface integral) of the target, are known. In the next Section 3, we will discuss the different scattering contributions to the RCS of a ship lying over the sea surface.

3. BISTATIC RADAR CROSS SECTION EVALUATION

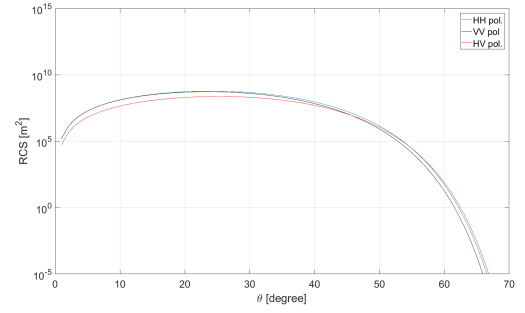
The scattering of a ship lying over the sea surface is mainly composed of *single-bounce* and *double-bounce* contributions (third-order terms can generally be neglected): the former is represented by the radar return from the ship deck and the sea surface [see pink solid and dashed lines, respectively, on Fig. 1(b)], whereas the latter are represented by the radar returns from the hull-to-sea and sea-to-hull reflections [see green solid and dashed lines, respectively, on Fig. 1(b)]. Here we focus on the double-bounce contributions, since, under KA-GO, the single-bounce term is significant only in the specular-point direction, as is clear from Fig. 1(b).

According to these considerations, a tool for the evaluation of the bistatic RCS of the ship is derived via the modeling of the double-bounce contributions and taking into account the ship orientation. Specifically, the following steps are performed for an accurate evaluation of the bistatic RCS, considering the hull-to-sea contribution only:

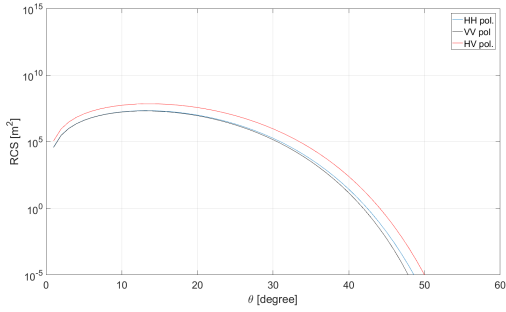
- 1) Material composition of the ship and physical parameters for the sea (e.g., temperature, salinity, wind speed, etc.) are acquired to calculate the corresponding dielectric constants and Fresnel coefficients using the approach in [1] and the Klein-Swift model, respectively.



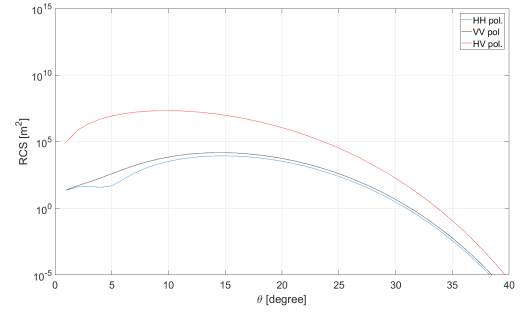
(a)



(b)

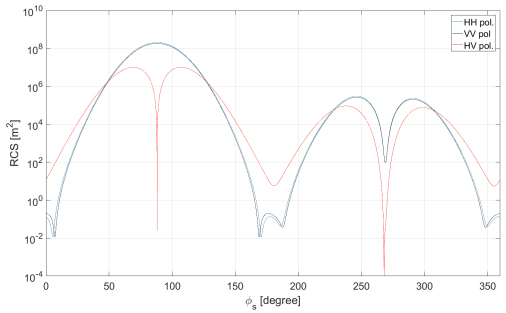


(c)

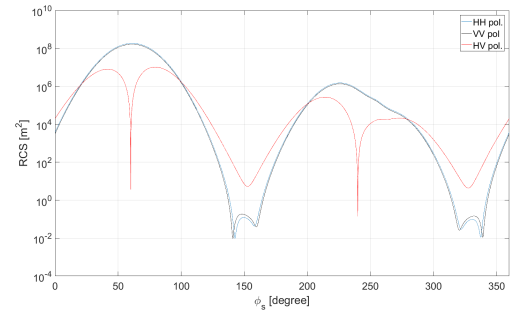


(d)

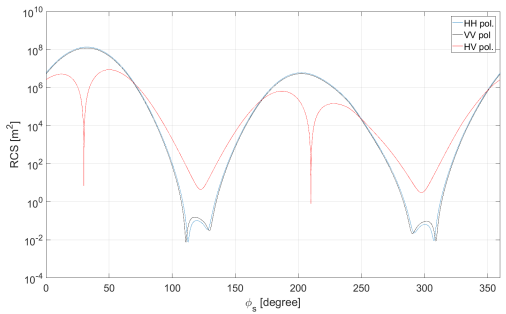
Fig. 2: Backscattering RCS of ship at 9 GHz for different orientation angles. (a) $\phi = 0^\circ$, (b) $\phi = 15^\circ$, (c) $\phi = 30^\circ$, (d) $\phi = 45^\circ$.



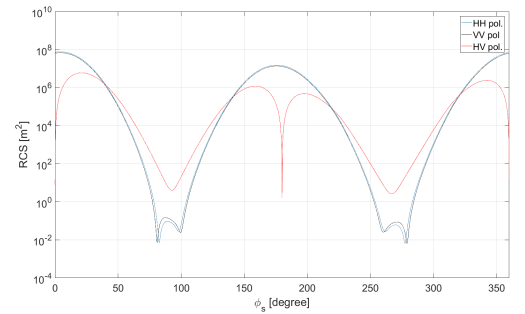
(a)



(b)



(c)



(d)

Fig. 3: RCS of the ship target at 1.5 GHz as a function of ϕ_s for (a) $\phi = 0^\circ$, (b) $\phi = 15^\circ$, (c) $\phi = 30^\circ$, (d) $\phi = 45^\circ$.

- 2) The transmitter and receiver positions are used to calculate the incident and receiver wave unit vectors, i.e., \hat{k}_i and \hat{k}_s , respectively.
- 3) The field scattered from the ship hull (first bounce) is well approximated by a plane wave under KA-GO due to the dimensions of the ship much larger w.r.t. the radar wavelength [7]. Only the scattering matrix for the first bounce (from the transmitter to the hull) must be evaluated. Since the boundary surface (i.e., the hull) is deterministic, the surface normal unit vector is known [see \hat{n}_h in Fig. 1(c)]. Therefore, the specular reflection condition is used to evaluate the scattered wavevector \hat{k}_{sp} (pointing towards the sea surface). The scattering coefficients are then evaluated once \hat{k}_i , \hat{k}_{sp} , and \hat{n}_h are determined.
- 4) The scattering matrix and the surface integral for the second bounce (from the sea surface to the receiver) are evaluated. Since the boundary surface (i.e., the sea) is random the surface normal unit vector \hat{n}_s is determined by the specular reflection condition, where now \hat{k}_{sp} plays the role of the incident wavevector [see Fig. 1(c)]. The scattering coefficients are then evaluated using the geometry of acquisition given by \hat{k}_{sp} , \hat{k}_s , and \hat{n}_s . Finally, the surface integral is evaluated for the considered acquisition geometry by numerical means and Monte Carlo method. Shading effects from the ship target are accounted for.
- 5) Equation (3) is used to evaluate the scattered field produced by the double-bounce reflection, by combining the results of points 3) and 4). More precisely, the overall scattering matrix is computed as the (non-commutative) product of the scattering matrix in 4) and that in 3). The surface integral is computed in 4).
- 6) The scattered field as calculated in 5) is used in Eq. (1) for final evaluation of the bistatic RCS.

The sea-to-hull contribution can be derived in a similar way following the previous steps.

4. NUMERICAL RESULTS

In this section, numerical results of the tool presented in the previous sections are reported. The dimensions of the simulated ship target are $250 \times 50 \times 10 \text{ m}^3$. Sea surface roughness is described via a 2-D Gaussian-Gaussian stochastic process with standard deviation $\sigma = 0.1 \text{ m}$, whereas its dielectric constant is evaluated via the Klein-Swift model with sea salinity 35 ppm, and temperature 19°C . The scattering integral over the sea surface has been evaluated by means of Monte Carlo simulation with 10^6 trials. Figures 2(a)-(d) show the RCS in backscattering configuration, i.e., azimuthal receiving angle $\phi_s = 90^\circ$ (see [7]), as a function of the radar look angle θ

for linear co-pol HH, VV, and cross-pol HV polarizations and assuming the aspect angle $\phi = 0^\circ$ (long side of ship facing the transmitter), $\phi = 15^\circ$, $\phi = 30^\circ$, and $\phi = 45^\circ$. It is noteworthy that larger values of the aspect angle ϕ give similar results due to the symmetry of the ship target. Cross-pol channel exhibits the lowest RCS values for small aspect angles and the highest RCS values for large aspect angles. Co-pol channels give similar results in the considered scenario. Figures 3(a)-(d) show the bistatic RCS as a function of the azimuth receiving angle ϕ_s for $\phi = 0^\circ$, $\phi = 15^\circ$, $\phi = 30^\circ$, and $\phi = 45^\circ$. Contributions from the different ship sides are clearly visible as local peaks of the RCS. The ship orientation dictates the angular position of such peaks. Finally, it is demonstrated that, for a large range of ship orientations, the backscattering acquisition geometry represents the most favorable configuration for ship detection applications in bistatic systems, such as GNSS-R.

5. REFERENCES

- [1] P. Iervolino, R. Guida, and P. Whittaker, "A model for the backscattering from a canonical ship in SAR imagery," *IEEE J. Sel. Topics Appl. Earth Observ. in Remote Sens.*, vol. 9, no. 3, pp. 1163–1175, 2016.
- [2] D. J. Crisp, "The state-of-the-art in ship detection in synthetic aperture radar imagery," Tech. Rep., Defence Science And Technology Organisation Salisbury (Australia) Info Sciences Lab, 2004.
- [3] A. Moreira and G. Krieger, "Spaceborne synthetic aperture radar (SAR) systems: state of the art and future developments," in *33rd Eur. Microw. Conf. (EuMC03)*. IEEE, 2003, vol. 1, pp. 101–104.
- [4] A. Di Simone, H. Park, D. Riccio, and A. Camps, "Sea target detection using spaceborne GNSS-R delay-doppler maps: Theory and experimental proof of concept using TDS-1 data," *IEEE J. Sel. Topics Appl. Earth Observ. in Remote Sens.*, vol. 10, no. 9, pp. 4237–4255, 2017.
- [5] M. P. Clarizia, P. Braca, C. S. Ruf, and P. Willett, "Target detection using GPS signals of opportunity," in *18th Int. Conf. Information Fusion (FUSION)*, Washington, DC, USA, July 6–9, 2015, pp. 1429–1436.
- [6] V. U. Zavorotny, S. Gleason, E. Cardellach, and A. Camps, "Tutorial on remote sensing using GNSS bistatic radar of opportunity," *IEEE Geosci. Remote Sens. Mag.*, vol. 2, no. 4, pp. 8–45, 2014.
- [7] G. Franceschetti, A. Iodice, and D. Riccio, "A canonical problem in electromagnetic backscattering from buildings," *IEEE Trans. Geosci. Remote Sens.*, vol. 40, no. 8, pp. 1787–1801, 2002.